Correlated electron–hole transitions in wurtzite GaN quantum dots: the effects of strain and hydrostatic pressure*

Zheng Dongmei(郑冬梅)†, Wang Zongchi(王宗篪), and Xiao Boqi(肖波齐)

Department of Physics and Electromechanical Engineering, Sanming College, Sanming 365004, China

Abstract: Within the effective-mass and finite-height potential barrier approximation, a theoretical study of the effects of strain and hydrostatic pressure on the exciton emission wavelength and electron–hole recombination rate in wurtzite cylindrical GaN/$Al_xGa_{1-x}N$ quantum dots (QDs) is performed using a variational approach. Numerical results show that the emission wavelength with strain effect is higher than that without strain effect when the QD height is large (> 3.8 nm), but the status is opposite when the QD height is small (< 3.8 nm). The height of GaN QDs must be less than 5.5 nm for an efficient electron–hole recombination process due to the strain effect. The emission wavelength decreases linearly and the electron–hole recombination rate increases almost linearly with applied hydrostatic pressure. The hydrostatic pressure has a remarkable influence on the emission wavelength for large QDs, and has a significant influence on the electron–hole recombination rate for small QDs. Furthermore, the present numerical outcomes are in qualitative agreement with previous experimental findings under zero pressure.

Key words: GaN quantum dots; excitons; strain; hydrostatic pressure

DOI: 10.1088/1674-4926/33/5/052002 **PACC:** 7320D; 7135

1. Introduction

Wide band-gap wurtzite III–V nitrides have been widely used in recent years in the design and fabrication of optical devices such as high-brightness blue/green light emitting diodes (LEDs)[1, 2] and laser diodes[3, 4]. Recently, it was found that the electronic and optical properties of wurtzite (WZ) GaN/AlGaN quantum heterostructures are affected by the built-in electric field (BEF) induced by the piezoelectricity and spontaneous polarizations. The magnitude of the BEF was estimated to be in the order of MV/cm[5, 6]. The exciton states and optical properties of strained GaN/$Al_xGa_{1-x}N$ heterostructures have been investigated[7−11]. These studies showed that a strong BEF leads to a remarkable reduction in the effective band-gap of the heterostructures and gives a significant spatial separation of the electrons and holes in the WZ GaN/AlGaN quantum heterostructures. However, none of these calculations included the strain dependence of the material parameters.

The hydrostatic pressure modifications of the physical properties of nitride-based low-dimensional structures are available and helpful for exploring new phenomena and improving devices[12, 13]. Wagner *et al.*[14] presented *ab initio* calculations of the structural, dielectric and lattice-dynamical properties of GaN and AlN under hydrostatic pressure. Goñi *et al.*[15] investigated, experimentally, the pressure modification of the phonon modes in wurtzite and zinc-blende GaN and wurtzite AlN. Lpkowski *et al.*[16] studied the influence of hydrostatic pressure on the light emission from a strained GaN/AlGaN multi-quantum-well system. It was found that the coefficient describing the pressure dependence of the photoluminescence peak energy was reduced with respect to the pressure dependence of the energy gap. This could be explained by the hydrostatic pressure-induced increase in the piezoelectric field in the quantum structures. Ha *et al.*[17] explored the influences of screening and hydrostatic pressure on the binding energies of heavy-hole excitons in a strained wurtzite GaN/$Al_{0.3}Ga_{0.7}N$ quantum well and obtained two important conclusions: (1) the binding energies of excitons increased almost linearly with pressure, and (2) the exciton binding energies increased obviously with decreasing barrier thickness due to the built-in electric field. To our knowledge, calculations of the interband optical transitions due to the excitons influenced by hydrostatic pressure in wurtzite GaN/$Al_xGa_{1-x}N$ cylindrical quantum dots (QDs) considering the strong BEF effect and strain dependence of material parameters, are still absent at present. In this paper we study, variationally, the effects of strain (including the strong BEF and the strain dependence of material parameters) and hydrostatic pressure on the interband optical transition and electron–hole recombination rate of heavy-hole excitons confined in a wurtzite GaN/$Al_xGa_{1-x}N$ cylindrical QD with finite height potential barriers.

2. Theoretical model

2.1. Variational calculation of the exciton states

Let us now consider an isolated cylindrical GaN QD with radius R and height L surrounded by a large energy gap material $Al_xGa_{1-x}N$, in which the origin is taken at the center of the QD and the z axis is defined to be the growth direction (see Fig. 1). Within the framework of effective mass, the Hamilto-

* Project supported by the National Natural Science Foundation of China (No. 11102100) and the Technology Projects of the Education Bureau of Fujian Province, China (No. JK2009038).

† Corresponding author. Email: smdmzheng@sina.com

Received 28 September 2011, revised manuscript received 2 December 2011

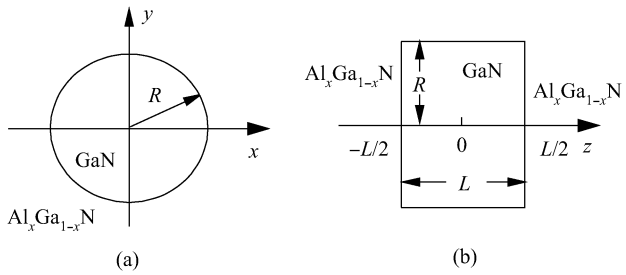

Fig. 1. A diagram of a wurtzite GaN cylindrical QD with radius R and height L surrounded by the large energy-gap material wurtzite $Al_xGa_{1-x}N$, in which the origin is taken at the center of the QD and the z axis is defined to be the growth direction.

nian of the exciton can be written as

$$\hat{H}_{ex} = \hat{H}_e + \hat{H}_h - \frac{e^2}{4\pi\varepsilon_0\bar{\varepsilon}\,|\boldsymbol{r}_e - \boldsymbol{r}_h|}, \tag{1}$$

where $\hat{H}_e$ ($\hat{H}_h$) is the electron (hole) Hamiltonian, $\boldsymbol{r}_e(\boldsymbol{r}_h)$ is the position vector of the electron (hole), e is the absolute value of the electron charge, ε_0 is the permittivity of free space, and $\bar{\varepsilon}$ is the effective mean relative dielectric constant of the embedding material between the electron and hole.

The Hamiltonian of the electron (hole) in the cylindrical coordinates reads

$$\hat{H}_j = -\frac{\hbar^2}{2m_j^*}\left[\frac{1}{\rho_j}\frac{\partial}{\partial\rho_j}\left(\rho_j\frac{\partial}{\partial\rho_j}\right) + \frac{1}{\rho_j^2}\frac{\partial^2}{\partial\varphi_j^2} + \frac{\partial^2}{\partial z_j^2}\right] + V(\rho_j) + V(z_j) \mp eEz_j, \tag{2}$$

where subscript j = e or h denotes the electron or hole and m_j^* is the electron (hole) effective mass. The sign $-(+)$ is for the electron (hole), and E is the BEF caused by the spontaneous and piezoelectric polarizations in the WZ $GaN/Al_xGa_{1-x}N$ QD. For infinitely wide barriers, the strength of E in the WZ $GaN/Al_xGa_{1-x}N$ QD is expressed as[10, 18]

$$\begin{cases} E^{GaN} = \left| -\dfrac{P_{sp}^{GaN}\hat{z} + P_{pE}^{GaN}\hat{z} - P_{sp}^{Al_xGa_{1-x}N}\hat{z}}{\varepsilon_e^{GaN}\varepsilon_0} \right|, \\ E^{Al_xGa_{1-x}N} \to 0, \end{cases} \tag{3}$$

where P_{sp}^{GaN}, P_{pE}^{GaN} and $P_{sp}^{Al_xGa_{1-x}N}$ are the spontaneous and piezoelectric polarizations of GaN and the spontaneous polarization of $Al_xGa_{1-x}N$, respectively, and ε_e^{GaN} is the electronic dielectric constant of the material GaN.

In Eq. (2), $V(\rho_j)$ and $V(z_j)$ are the in-plane and z-direction confinement potential due to the band offset (Q_j) in the WZ $GaN/Al_xGa_{1-x}N$ QD, respectively. They can be given by

$$V(\rho_j) = \begin{cases} 0, & \rho_j \leqslant R, \\ Q_j\left[E_g(Al_xGa_{1-x}N) - E_g(GaN)\right], & \rho_j > R, \end{cases} \tag{4}$$

$$V(z_j) = \begin{cases} 0, & |z_j| \leqslant \dfrac{L}{2}, \\ Q_j\left[E_g(Al_xGa_{1-x}N) - E_g(GaN)\right], & |z_j| > \dfrac{L}{2}. \end{cases} \tag{5}$$

In this paper, the ratio of the conduction band to the valence band offset is assumed to be 75 : 25[19].

The wave function of the electron (hole) confined in the WZ $GaN/Al_xGa_{1-x}N$ QD can be written as

$$\psi_j(\rho_j, \varphi_j, z_j) = f(\rho_j)h(z_j)e^{im\varphi_j}, \quad m = 0, \pm1, \pm2, \cdots, \tag{6}$$

where m is the electron (hole) z-component angular momentum quantum number. The radial wave function $f(\rho_j)$ of the electron (hole) can be obtained using the Bessel function J_m and the modified Bessel function K_m. Wave function $h(z_j)$ can be expressed by means of the Airy functions A_i and B_i.

In order to calculate the exciton binding energy, the trial wave function can be chosen as[10,20−22]

$$\Phi_{ex}(\boldsymbol{r}_e, \boldsymbol{r}_h) = \psi_e(\rho_e, \varphi_e, z_e)\,\psi_h(\rho_h, \varphi_h, z_h)\,e^{-\alpha\rho_{eh}^2}e^{-\beta z_{eh}^2}, \tag{7}$$

where ψ_e (ψ_h) is the electron (hole) wave function confined in the QD, $\rho_{eh}^2 = \rho_e^2 + \rho_h^2 - 2\rho_e\rho_h\cos(\varphi_e - \varphi_h)$, $z_{eh}^2 = (z_e - z_h)^2$, and α and β are variational parameters.

The ground-state energy of the exciton can be determined by

$$E_{ex} = \min_{\alpha,\beta}\frac{\left\langle \Phi_{ex} \middle| \hat{H}_{ex} \middle| \Phi_{ex} \right\rangle}{\langle \Phi_{ex} \mid \Phi_{ex} \rangle}. \tag{8}$$

The exciton binding energy E_b and the optical transition energy E_{ph} can be defined as follows,

$$E_b = E_e + E_h - E_{ex}, \tag{9}$$

$$E_{ph} = E_g + E_e + E_h - E_b, \tag{10}$$

where E_g is the effective band-gap energy of the GaN material, and E_e (E_h) is the electron (hole) confinement energy in the QD.

The emission wavelength associated with the exciton can be represented as

$$\lambda = \frac{hc}{E_g + E_{ex}}. \tag{11}$$

The probability of radiative transition associated with the exciton states described by the wave function (Eq. (7)) is proportional to the square of the overlap integral defined as[20]

$$M_{e-h}^2 = \left| \int d\boldsymbol{r}_e d\boldsymbol{r}_h \Phi_{ex}(\boldsymbol{r}_e, \boldsymbol{r}_h)\delta(\boldsymbol{r}_e - \boldsymbol{r}_h) \right|^2. \tag{12}$$

2.2. Pressure and strain dependence of the parameters

The pressure- and strain-dependent energy gaps of GaN and AlN are[23]

$$E_{g,GaN} = E_{g,GaN}(P) + 2(a_{2,GaN} + b_{2,GaN})\varepsilon_{xx,GaN} + (a_{1,GaN} + b_{1,GaN})\varepsilon_{zz,GaN}, \tag{13}$$

$$E_{g,AlN} = E_{g,AlN}(P) + 2a_{2,AlN}\varepsilon_{xx,AlN} + a_{1,AlN}\varepsilon_{zz,AlN}, \tag{14}$$

where $a_{1,i}$, $a_{2,i}$, $b_{1,i}$ and $b_{2,i}$ (i = GaN or AlN) are the deformation potentials. The dependence of the energy gap on hydrostatic pressure P is considered by the following equation[17]

$$E_{g,i}(P) = E_{g,i}(0) + \chi_i P. \tag{15}$$

The energy gap of the ternary mixed crystal $Al_xGa_{1-x}N$ (chosen as the barriers) is[19]:

$$E_{g,Al_xGa_{1-x}N} = E_{g,GaN}(1-x) + E_{g,AlN}x - 1.3(\text{eV})x(1-x). \tag{16}$$

Within the infinitely thick barrier approximation, the biaxial lattice-mismatch induced strains in the GaN QD are given as[24]

$$\varepsilon_{xx,GaN} = \varepsilon_{yy,GaN} = \frac{a_{AlGaN}(P) - a_{GaN}(P)}{a_{GaN}(P)}, \tag{17}$$

where $a_{AlGaN}(P)$ and $a_{GaN}(P)$ represent the a-axis lattice constant of $Al_xGa_{1-x}N$ and GaN. The lattice constant as a function of hydrostatic pressure is given by[25]

$$a_i(P) = a_{0i}\left(1 - \frac{P}{3B_{0i}}\right), \tag{18}$$

where superscript i = w or b donates the well or barrier materials. The bulk modulus B_{0i} in a wurtzite structure is given by elastic constants C_{11}, C_{12}, C_{13} and C_{33} as[24]

$$B_{0i} = \frac{(C_{11,i} + C_{12,i})C_{33,i} - 2C_{13,i}^2}{C_{11,i} + C_{12,i} + 2C_{33,i} - 4C_{13,i}}. \tag{19}$$

Based on the Hooke's law, the ratio of the in-plane strain component and the strain component along the c axis can be expressed by[24]

$$\frac{\varepsilon_{zz,i}}{\varepsilon_{xx,i}} = \frac{C_{11,i} + C_{12,i} - 2C_{13,i}}{C_{33,i} - C_{13,i}}. \tag{20}$$

The strain and hydrostatic pressure dependences of the effective masses of an electron in the z direction and the x–y plane can be calculated by[26]

$$\frac{m_0}{m_{e,i}^{\perp,//}(P)} = 1 + \frac{C}{E_{g,i}}. \tag{21}$$

Here, C is a constant and can be determined by solving Eq. (21) at $P = 0$. In general, the pressure coefficient for a heavy-hole is assumed to be zero.

Static dielectric constant ε_s is influenced by the strain and hydrostatic pressure, respectively. The tensor components of ε_s for the wurtzite structure are derived from the generalized Lyddane–Sachs–Teller relation[24]

$$\varepsilon_{s,\delta\delta} = \varepsilon_{\infty,\delta\delta}\left(\frac{\omega_{LO,\delta\delta}}{\omega_{TO,\delta\delta}}\right)^2. \tag{22}$$

The frequencies of LO and TO phonons influenced by pressure and strain in Eq. (22) can be written as[24]

$$\omega_{j,\delta\delta} = \omega_{j,\delta\delta}(P) + 2K_{j,xx}\varepsilon_{xx} + K_{j,zz}\varepsilon_{zz}, \tag{23}$$

where $K_{j,xx}$ and $K_{j,zz}$ are the strain coefficients of the phonon modes given in Ref. [24], and j represents the LO or TO phonon. The tensor component ($\delta = z, x$) is related to the LO and TO phonon frequencies, respectively. Furthermore, the hydrostatic pressure dependence of $\omega_{j,\delta\delta}(P)$ can be determined by the given mode Grüneisen parameter[27]:

$$\gamma_{j,\delta\delta} = B_0\frac{1}{\omega_{j,\delta\delta}} \times \frac{\partial\omega_{j,\delta\delta}(P)}{\partial P}. \tag{24}$$

Considering the influence of hydrostatic pressure, the high-frequency dielectric constant in Eq. (22) can be written as[28]

$$\frac{\partial\varepsilon_{\infty,\delta\delta}(P)}{\partial P} = -\frac{5(\varepsilon_{\infty,\delta\delta} - 1)}{3B_0}(0.9 - f_{ion}), \tag{25}$$

where f_{ion} is the ionicity of the material under pressure.

The effective mean relative dielectric constant in Eq. (1) is defined as

$$\bar{\varepsilon}(P) = \frac{2}{3}\varepsilon_{s,xx}(P) + \frac{1}{3}\varepsilon_{s,zz}(P). \tag{26}$$

The strain-induced piezoelectric polarization in Eq. (3) is written as[29]

$$P_{pE}^{GaN} = 2e_{31}(P)\varepsilon_{xx} + e_{33}(P)\varepsilon_{zz}, \tag{27}$$

where e_{31} and e_{33} are the strain-dependent piezoelectric constants of GaN satisfying[29]

$$e_{31}(P) = e_{31}(0) + \frac{4Z^*e}{\sqrt{3}a_{GaN}^2(P)}\frac{d\mu}{d\varepsilon_{xx}}, \tag{28}$$

$$e_{33}(P) = e_{33}(0) + \frac{4Z^*e}{\sqrt{3}a_{GaN}^2(P)}\frac{d\mu}{d\varepsilon_{zz}}, \tag{29}$$

where $e_{31}(0)$ and $e_{33}(0)$ are the clamped-ion terms that represent the effects of strain on the electronic structure, and the second term in Eqs. (28) and (29) is the contribution resulting from the relative displacement of the anion and cation sublattices (internal strain term). The other quantities in Eqs. (28) and (29) are the Born effective charge Z^* along the c axis, the lattice constant $a_{GaN}(P)$ of GaN, and the internal parameter u. From Ref. [24], we can obtain Z^* =1.18, $\frac{d\mu}{d\varepsilon_{zz}} = -0.208$, $\frac{d\mu}{d\varepsilon_{xx}} = 0.262$.

The pressure-dependent radius and height of the GaN QD may be obtained from the fractional change in volume associated with the hydrostatic pressure[30],

$$\frac{\Delta V}{V_0} = -3P(S_{11} + 2S_{12}), \tag{30}$$

with $V(P) = \pi R^2(P)L(P)$, $V_0 = \pi R_0^2 L_0$, $\Delta V = V(P) - V_0$, and therefore

$$R(P) = R_0[1 - 3P(S_{11} + 2S_{12})]^{1/3}, \tag{31}$$

$$L(P) = L_0[1 - 3P(S_{11} + 2S_{12})]^{1/3}, \tag{32}$$

where R_0 (L_0) is the radius (height) of the QD at atmospheric pressure, and S_{11} and S_{12} are the compliance constants of GaN given by[30]

$$S_{11} = \frac{(C_{11,GaN} + C_{12,GaN})}{[(C_{11,GaN} - C_{12,GaN})(C_{11,GaN} + 2C_{12,GaN})]}, \tag{33}$$

$$S_{12} = \frac{-C_{12,GaN}}{[(C_{11,GaN} - C_{12,GaN})(C_{11,GaN} + 2C_{12,GaN})]}. \tag{34}$$

Table 1. Physical parameters of wurtzite GaN and AlN used in the computation.

	a (nm)	C_{11} (GPa)	C_{12} (GPa)	C_{13} (GPa)	C_{33} (GPa)	e_{31} (C/m^2)	e_{33} (C/m^2)	P^{SP} (C/m^2)
GaN	0.3189[a]	390[b]	145[b]	106[b]	398[b]	–0.49[c]	0.73[c]	–0.029[c]
AlN	0.3112[a]	398[b]	140[b]	127[b]	382[b]			–0.081[c]

[a]Ref. [31]. [b]Ref. [32]. [c]Ref. [33].

Table 2. The other physical parameters of wurtzite GaN and AlN used in the computation.

	E_g (meV)	$m_e^*(m_0)$	χ (meV/GPa)	f_{ion}	a_1 (meV)	a_2 (meV)	b_1 (meV)	b_2 (meV)
GaN	3507[a]	0.2[a]	33[b]	0.5[c]	–4090[d]	–8870[d]	–7020[d]	3650[d]
AlN	6230[a]	0.32[a]	43[b]	0.499[c]	–3390[d]	–11810[d]	–9420[d]	4020[d]

[a]Ref. [31]. [b]Ref. [34]. [c]Ref. [17]. [d]Ref. [24].

Table 3. The other physical parameters of wurtzite GaN and AlN used in the computation.

	$\varepsilon_{\infty,xx}$	$\varepsilon_{\infty,zz}$	$\omega_{LO,xx}$ (cm^{-1})	$\omega_{LO,zz}$ (cm^{-1})	$\omega_{TO,xx}$ (cm^{-1})	$\omega_{TO,zz}$ (cm^{-1})	$\gamma_{LO,xx}$	$\gamma_{LO,zz}$	$\gamma_{TO,xx}$	$\gamma_{TO,zz}$
GaN	5.20[a]	5.39[a]	757[b]	748[b]	568[b]	541[b]	0.99[b]	0.98[b]	1.19[b]	1.21[b]
AlN	4.30[a]	4.52[a]	924[b]	898[b]	677[b]	618[b]	0.91[b]	0.82[b]	1.18[b]	1.02[b]

[a]Ref. [24]. [b]Ref. [14].

Table 4. Calculated and measured optical transition energies under zero hydrostatic pressure in GaN/$Al_xGa_{1-x}N$ QDs. For comparison, the results calculated by Dai *et al.* without considering the strain dependence of the material parameters are also listed.

L (nm)	R (nm)	x	E_{ph}^{expt} (eV)	E_{ph}^{calc} (eV)		Error (%)	
				Present	Dai	Present	Dai
3.5	5	0.15	3.581[a]	3.560	3.509[b]	0.59	2[b]
5.5	25	0.10	3.440[c]	3.443	3.414[b]	0.09	0.7[b]

[a]Ref. [19]. [b]Ref. [10]. [c]Ref. [35].

3. Numerical results and discussion

We calculated the emission wavelengths and the electron-hole recombination rates in WZ GaN/$Al_xGa_{1-x}N$ cylindrical QDs with finite height potential barriers by considering strain and hydrostatic pressure effects. For simplicity, we concentrated on the heavy-hole exciton states in the following. All the material parameters used in our calculations are listed in Tables 1–3.

A comparison between the theoretical and measured optical transition energies under zero hydrostatic pressure is presented in Table 4. The good agreement between the present theoretical results and the previous experimental ones suggests that the models are suitable for investigating excitonic properties in GaN QD nanostructures. Comparison with the results calculated by Dai *et al.*[10] without considering the strain dependence of material parameters, one can see that the strain dependence of the material parameters isn't ignorable, especially for the small QDs with a large Al content.

Figure 2 shows the emission wavelength and the electron-hole recombination rate as a function of the QD height in GaN/$Al_{0.15}Ga_{0.85}N$ QDs with a radius $R = 5$ nm under zero hydrostatic pressure. Curve A is with a BEF and strain dependence of the physical parameters, curve B is without strain effect, curve C is with a BEF only, and curve D is with strain dependence of the physical parameters only. From Fig. 2(a) we can see that as the QD height increases, the emission wavelength monotonically increases in all cases. This is because the energies of the non-correlated confined electron and hole states reduce with the increase in the QD height. Thus, the ground-state energy of the exciton decreases, and the emission wavelength increases. It can be further noted that the emission wavelength is significantly increased by BEF if L increases (see curves B and C). The result can be explained by the redshift of the effective band-gap of the GaN layer due to the strong BEF. It is also seen that the strain dependence of the material parameters leads to the decrease in the emission wavelength and has a remarkable influence on the emission wavelength for the QDs with small height L (see curves B and D). Furthermore, comparing curve A with curve B, the emission wavelength with strain effect is higher than that without strain effect when the QD height is > 3.8 nm, but the emission wavelength with strain effect becomes lower than that without strain effect as the QD height is < 3.8 nm.

Moreover, we can clearly see from Fig. 2(b) that the electron-hole recombination rate reduces quickly with an increase in the QD L height, if considering the BEF (curves A and C). The reason is that the electron–hole spatial separation in the z-direction is enlarged due to the BEF when L increases. For a large L height ($L \geqslant 5.5$ nm), Figure 2(b) shows that the electron–hole recombination rate approaches almost zero. Therefore, the height of GaN QDs must be less than 5.5 nm for an efficient electron–hole recombination process. This finding is extremely important for QD device applications. Comparing to the electron–hole recombination rate without BEF (curves B and D), we can see that the BEF may reduce the electron–hole

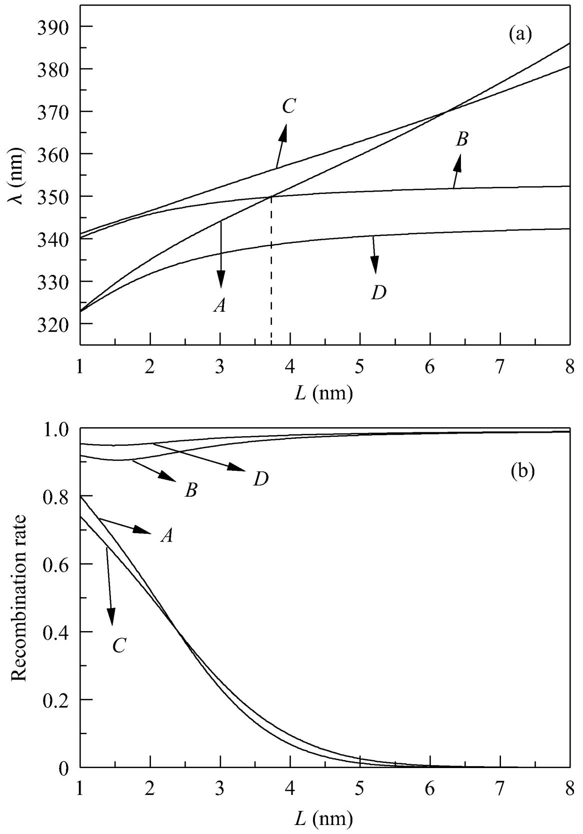

Fig. 2. (a) Emission wavelength λ and (b) the electron–hole recombination rate as a function of the QD height in $GaN/Al_{0.15}Ga_{0.85}N$ QDs with radius $R = 5$ nm under zero hydrostatic pressure. Curve A is with built-in electric field and strain dependence of the physical parameters, curve B is without strain effect, curve C is only with built-in electric field, and curve D is only with strain dependence of the physical parameters.

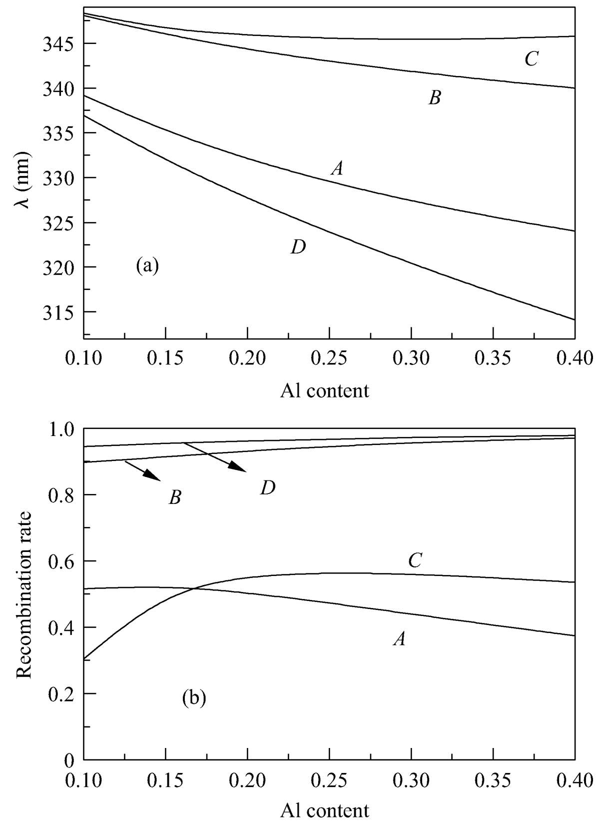

Fig. 3. (a) Emission wavelength λ and (b) the electron–hole recombination rate as a function of the Al content in $GaN/Al_xGa_{1-x}N$ QDs with height $L = 2$ nm and radius $R = 5$ nm under zero hydrostatic pressure. The curves A, B, C and D have the same meaning as in Fig. 2.

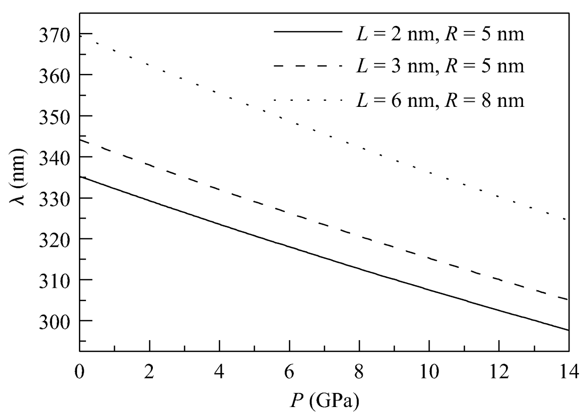

Fig. 4. Emission wavelength λ in strained $GaN/Al_{0.15}Ga_{0.85}N$ QDs as a function of the hydrostatic pressure for different QD sizes.

recombination rate greatly. Comparing curve B with curve D, we note that the strain dependence of the material parameters induces the increase in the recombination rate and has a remarkable influence for the QDs with a small L height.

In Fig. 3, the emission wavelength λ and the electron–hole recombination rate are further investigated as a function of Al content x in $GaN/Al_xGa_{1-x}N$ QDs with height $L = 2$ nm and radius $R = 5$ nm under zero hydrostatic pressure. Curve A is with BEF and strain dependence of the physical parameters, curve B is without strain effect, curve C is only with BEF, and curve D is only with strain dependence of the physical parameters. Comparing curve B with curve C in Fig. 3(a), we can see that the strong BEF gives rise to an increase in the emission wavelength when the Al content is increased. Figure 3(a) also shows that the strain dependence of the material parameters leads to a large decrease in the emission wavelength, and has a remarkable influence on the QDs with large Al content (see curves B and D). The interaction of these two effects induces the emission wavelength with strain effect to become lower than that without strain effect, especially for the QDs with a large Al content (see curves A and B). This result coincides with the one obtained from Fig. 2(a). In particular, from Fig. 3(b) we can clearly see that the BEF greatly reduces the electron-hole recombination rate (see curves B and C). And the strain dependence of the material parameters obviously increases the recombination rate when the Al content is less (see curves B and D). The interaction of these two effects slowly diminishes the electron-hole recombination rate with strain effect, with increasing Al content (curve A).

Figure 4 gives the emission wavelength λ in strained WZ $GaN/Al_{0.15}Ga_{0.85}N$ cylindrical QDs as a function of the hydrostatic pressure. It shows that the emission wavelength linearly decreases with increasing hydrostatic pressure. The pressure-related changes are mainly due to the pressure dependence of both the energy gap of GaN and the QD volume. The behav-

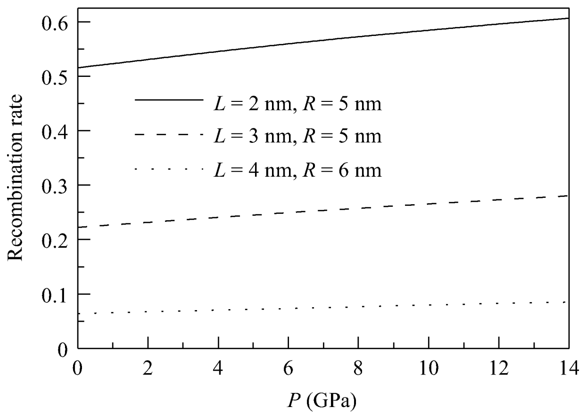

Fig. 5. Electron–hole recombination rate in strained GaN/$Al_{0.15}Ga_{0.85}N$ QDs as a function of the hydrostatic pressure for different QD sizes.

ior is as follows. As the pressure increases: (1) the energy gap of GaN increases, and (2) the QD volume decreases leading to an increase in the exciton ground-state energy. These two effects induce the increase in the effective band-gap of the GaN layer, and thus the emission wavelength decreases, and the pressure has a remarkable influence on the emission wavelength for large QDs. For example, at $L = 6$ nm and $R = 8$ nm, the reduction in the emission wavelength is 44.99 nm as the pressure increases from 0 to 14 GPa. At $L = 3$ nm and $R = 5$ nm, the corresponding reduction in the emission wavelength is 39.14 nm. Whereas the corresponding decrease in the emission wavelength is 37.49 nm when the QD height $L = 2$ nm and radius $R = 5$ nm.

Figure 5 shows the electron–hole recombination rate in a strained WZ GaN/$Al_{0.15}Ga_{0.85}N$ cylindrical QD as a function of the hydrostatic pressure. It indicates that the electron–hole recombination rate increases approximately linearly with increasing hydrostatic pressure. This is because the electron–hole spatial separation reduces with increasing hydrostatic pressure. From Fig. 5, we can see that the pressure has a significant influence on the electron-hole recombination rate for a small QD.

4. Conclusions

We investigated the effects of strain and hydrostatic pressure on the emission wavelength and electron–hole recombination rate in wurtzite GaN/$Al_xGa_{1-x}N$ cylindrical QDs with finite potential barriers. Calculations are performed via a variational procedure within the effective-mass approximation. Numerical results show that the strain dependence of the material parameters leads to a decrease in the emission wavelength and an increase in the electron–hole recombination rate. The strong BEF gives rise to an increase in the emission wavelength and a large reduction in the electron–hole recombination rate. The interaction of these two effects leads to an emission wavelength with strain effect that is higher than that without strain effect when the QD height is > 3.8 nm, but the opposite of this occurs when the QD height is < 3.8 nm. The height of GaN QDs must be less than 5.5 nm for an efficient electron–hole recombination process due to the strain effect. The emission wavelength decreases linearly and the electron–hole recombination rate increases almost linearly with applied hydrostatic pressure. The hydrostatic pressure has a remarkable influence on the emission wavelength for large QDs, and a significant influence on the electron–hole recombination rate for small QDs. Furthermore, our numerical outcomes are in qualitative agreement with previous experimental findings under zero pressure.

References

[1] Nakamura S, Chichibu S F. Introduction to nitride semiconductor blue lasers and light emitting diodes. London: Taylor & Francis, 2000

[2] Mukai T, Narimatsu H, Nakamura S. Amber InGaN-based light-emitting diodes operable at high ambient temperatures. Jpn J Appl Phys II, 1998, 37: L479

[3] Akasaki I, Sota S, Sakai H, et al. Shortest wavelength semiconductor laser diode. Electron Lett, 1996, 32: 1105

[4] Nakamura S, Senoh M, Nagahama S, et al. Violet InGaN/GaN/AlGaN-based laser diodes operable at 50 ℃ with a fundamental transverse mode. Jpn J Appl Phys II, 1999, 38: L226

[5] Bernardini F, Fiorentini V. Electronic dielectric constants of insulators calculated by the polarization method. Phys Rev B, 1998, 58: 15292

[6] Bernardini F, Fiorentini V, Vanderbilt D. Polarization-based calculation of the dielectric tensor of polar crystals. Phys Rev Lett, 1997, 79: 3958

[7] Fonoberov V A, Balandin A A. Excitonic properties of strained wurtzite and zinc-blende GaN/$Al_xGa_{1-x}N$ quantum dots. J Appl Phys, 2003, 94: 7178

[8] Bretagnon T, Kalliakos S, Lefebvre P, et al. Time dependence of the photoluminescence of GaN/AlN quantum dots under high photoexcitation. Phys Rev B, 2003, 68: 205301

[9] De Rinaldis S, Amico I D, Rossi F. Intrinsic electric field effects on few-particle interactions in coupled GaN quantum dots. Phys Rev B, 2004, 69: 235316

[10] Dai X Q, Huang F Z, Zheng D M. Influence of Al content on exciton confined in GaN/$Al_xGa_{1-x}N$ quantum dots. Chinese Journal of Semiconductors, 2005, 26: 697 (in Chinese)

[11] Zheng D M, Dai X Q. Exciton states confined in strained GaN/$Al_xGa_{1-x}N$ quantum dots. Journal of Huaibei Coal Industry Teachers College (Natural Science Edition), 2006, 27: 31 (in Chinese)

[12] Ha S H, Ban S L. Binding energies of screened excitons in a strained (111)-oriented Zinc-blend GaN/AlGaN quantum well under hydrostatic pressure. Journal of Semiconductors, 2008, 29: 234

[13] Zhang M, Ban S L. Pressure influence on bound polarons in a strained wurtzite GaN/$Al_xGa_{1-x}N$ heterojunction under an electric field. Journal of Semiconductors, 2010, 31: 052002

[14] Wagner J M, Bechstedt F. Pressure dependence of the dielectric and lattice-dynamical properties of GaN and AlN. Phys Rev B, 2000, 62: 4526

[15] Goñi A R, Siegle H, Syassen K, et al. Effect of pressure on optical phonon modes and transverse effective charges in GaN and AlN. Phys Rev B, 2001, 64: 035205

[16] Lpkowski S P, Teisseyre H, Suski T, et al. Piezoelectric field and its influence on the pressure behavior of the light emission from GaN/AlGaN strained quantum wells. Appl Phys Lett, 2001, 79: 1483

[17] Ha S H, Ban S L. Binding energies of excitons in a strained wurtzite GaN/AlGaN quantum well influenced by screening and hydrostatic pressure. J Phys: Condens Matter, 2008, 20: 085218

[18] Xia C X, Wei S Y, Zhao X. Built-in electric field effect on hydrogenic impurity in wurtzite GaN/AlGaN quantum dot. Appl Surf

Sci, 2007, 253: 5345
[19] Ramvall P, Tanaka S, Nomura S, et al. Observation of confinement-dependent exciton binding energy of GaN quantum dots. Appl Phys Lett, 1998, 73: 1104
[20] Shi J J, Gan Z Z. Effects op piezoelectricity and spontaneous polarization on localized excitons in self-formed InGaN quantum dots. J Appl Phys, 2003, 94: 407
[21] Szafran B, Bednarek S, Adamowski J. Parity symmetry and energy spectrum of excitons in coupled self-assembled quantum dots. Phys Rev B, 2001, 64: 125301
[22] Li S S, Xia J B, Yuan Z L, et al. Effective-mass theory for InAs/GaAs strained coupled quantum dots. Phys Rev B, 1996, 54: 11575
[23] Shan W, Hauenstein R J, Fischer A J, et al. Strain effects on excitonic transitions in GaN: deformation potentials. Phys Rev B, 1996, 54: 13460
[24] Wagner M, Bechstedt F. Properties of strained wurtzite GaN and AlN: *ab initio* studies. Phys Rev B, 2002, 66: 115202
[25] Perlin P, Mattos L, Shapiro N A, et al. Reduction of the energy gap pressure coefficient of GaN due to the constraining presence of the sapphire substrate. J Appl Phys, 1999, 85: 2385
[26] Ting D Z Y, Chang Y C. Γ–X mixing in GaAs/$Al_xGa_{1-x}As$ and $Al_xGa_{1-x}As$/AlAs superlattices. Phys Rev B, 1987, 36: 4359
[27] Holtz M, Seon M, Brafman O, et al. Pressure dependence of the optic phonon energies in $Al_xGa_{1-x}As$. Phys Rev B, 1996, 54: 8714
[28] Goñi A R, Syassen K, Cardona M. Effect of pressure on the refractive index of Ge and GaAs. Phys Rev B, 1990, 41:10104
[29] Vaschenko G, Patel D, Menoni C S, et al. Significant strain dependence of piezoelectric constants in $In_xGa_{1-x}N$/GaN quantum wells. Phys Rev B, 2001, 64: 241308
[30] Raigoza N, Duque C A, Porras-Montenegro N, et al. Correlated electron hole transition energies in quantum-well wires: effects of hydrostatic pressure. Physica B, 2006, 371: 153
[31] Vurgaftman I, Meyer J R, Ram-Mohan L R. Band parameters for III–V compound semiconductors and their alloys. J Appl Phys, 2001, 89: 5815
[32] Park S H, Chuang S L. Comparison of zinc-blende and wurtzite GaN semiconductors with spontaneous polarization and piezoelectric field effects. J Appl Phys, 2000, 87: 353
[33] Bernardini F, Fiorentini V, Vanderbilt D. Spontaneous polarization and piezoelectric constants of III–V nitrides. Phys Rev B, 1997, 56: R10024
[34] Wei S H, Zunger A. Predicted band-gap pressure coefficient of all diamond and zinc-blende semiconductors: chemical trends. Phys Rev B, 1999, 60: 5404
[35] Tanaka S, Lee J S, Ramvall P, et al. A UV light-emitting diode incorporating GaN quantum dots. Jpn J Appl Phys, 2003, 42: L885